Korean J. Chem. Eng., **16**(4), 441-448 (1999)

A Mathematical Model for Unsteady-State Oxygen Transfer in an External-Loop Airlift Reactor

Keun Ho Choi†

Department of Chemical Engineering, Taejon National University of Technology,
305, Samsung-dong, Dong-gu, Taejon 300-717, Korea
(*Received 19 November 1998 • accepted 6 April 1999*)

Abstract–A mathematical model for simulation of unsteady-state oxygen transfer in an external-loop airlift reactor was developed. The airlift reactor was represented by a number of interconnected tanks, each of which was assumed to be well mixed. The effect of gas circulation rate on the oxygen transfer was considered. The model can be used for the determination of mass transfer performance of the airlift reactor in which the whole liquid phase cannot be assumed to be fully back-mixed. The simulation results showed a good agreement with experimental results.

Key words : External-Loop Airlift Reactor, Unsteady-State Oxygen Transfer, Gas Circulation Rate

INTRODUCTION

Mass transfer coefficients in laboratory and industrial equipment can be measured by either steady-state or unsteady-state mass transfer experiments. In the case of gas absorption in a batch system, steady-state experiments are associated with a sink for absorbed gas by means of chemical reactions. Since reactive solutes in the liquid may severely influence the physical properties of the system, the generality of the experimental results is largely restricted to the system being studied. Therefore, oxygen transfer coefficients for a particular absorption unit are usually determined by dynamic method which can avoid the complication with reactions. The method simplifies comparing oxygen transfer efficiencies in different types of equipment.

The dynamic method is based on the comparison of a measured value of dissolved oxygen concentration with the calculated value by a mathematical model. The choice of model is very important because poor assumptions of hydrodynamic characteristics of the equipment may lead to erroneous results. In numerous investigations [Weiland and Onken, 1981; Muroyama et al., 1985; Chisti and Moo-Young, 1988; Siegel and Merchuk, 1988; Choi et al., 1990; Choi, 1993] on the oxygen transfer capability of airlift reactors, the composition in gas phase was assumed to be constant, and the liquid phase was considered to be fully back-mixed. In other words, most of data for mass transfer coefficients are based on the assumption that the reactor is a single unit, rather than composed of discrete sections. We call it a well-mixed model. In the case of most small airlift reactors, the well-mixed model is used for the determination of volumetric mass transfer coefficients for two reasons : one, that the assumptions are valid in the reactors ; two, the simplicity of the model.

Unsteady state methods of determining mass transfer coefficients are complicated by the possibility of distortion of the measured values by the probe response dynamics. Probe response dynamics will become an influential factor in mass transfer coefficient calculations when the value for mass transfer coefficient is approximately equal to or greater than the inverse of the probe response time [Merchuk and Siegel, 1988]. Weiland and Onken [1981] assumed perfect mixing in both the liquid and gas phases. They also considered the lag in the electrode response due to the oxygen probe dynamics. So, they suggested a well-mixed model as follows:

$$\frac{C_L^*-C_{Lp}}{C_L^*-C_{Lo}}=\left[\frac{\exp(-K_La_L\cdot t)}{t_e}-K_La_L\cdot\exp(-t/t_e)\right]\frac{t_e}{1-K_La_L\cdot t_e} \quad (1)$$

Ho et al. [1977] represented a concentric airlift reactor as a tank-in-series model having a number of interconnected compartments, each of which was assumed to be well mixed. In the model, the top section was considered to be well mixed. The axial dispersion in the gas phase was assumed to be identical to the axial dispersion in the liquid phase. The model was used to simulate steady-state oxygen transfer in an airlift fermenter.

Merchuk and Stein [1980] introduced a distributed parameter model for oxygen transfer in a split airlift reactor. They assumed that the flows in both gas and liquid phases in the riser behaved like a plug flow. They regarded the top section as a well-mixed tank. The downcomer was also considered as a plug flow of liquid phase only.

Luttmann et al. [1982] analyzed mass transfer data for an external-loop airlift fermenter based on a distribution parameter model. The model did not take into account the possibility of mass transfer in the downcomer, probably because the volume fraction of the downcomer to the total reactor volume was very small. The model does not fit for airlift reactors with large amounts of gas circulation.

Based on computer simulation results obtained by the unsteady-state mixing model, Andre et al. [1983] developed a simple criterion that specifies the conditions for the validity of the well-mixed model in practice. In order to represent the back-mixing

†To whom correspondence should be addressed.
E-mail : khchoi@hyunam.tnut.ac.kr

in the liquid and gas phases, they also used a tank-in-series model for both the riser and the downcomer. However, the circulation of the gas phase and the interphase mass transfer in the downcomer were not considered.

In this study, a mathematical model considering both the effect of the gas circulation rate and the role of the downcomer in oxygen transfer was developed for the simulation of unsteady-state oxygen transfer in an external-loop airlift reactor.

THEORY

A typical external-loop airlift consists of a riser, a downcomer, two connection sections, a top section above the riser, and a top section above the downcomer as shown in Fig. 1. In the present study, a tanks-in-series model is used for both liquid and gas phases in the riser and the circulation loop which includes the two connections and the downcomer because the oxygen concentrations in both phases vary with time and position in the reactor. A schematic diagram of the unsteady-state mass transfer model for an external-loop airlift reactor is presented in Fig. 2. It is assumed that complete mixing prevails for each phase in interconnected tanks. Back-mixing for liquid phase in the riser and the circulation loop is represented by M_L and N_L stages, respectively. Back-mixing for gas phase in the riser and the circulation loop is represented by M_G and N_G stages, respectively. In practice, the extent of back-mixing in the gas phase is not necessarily identical to that in the liquid phase. The number of stages, i.e., M_L, N_L, M_G and N_G, can be adjusted, based on the extent of axial dispersion.

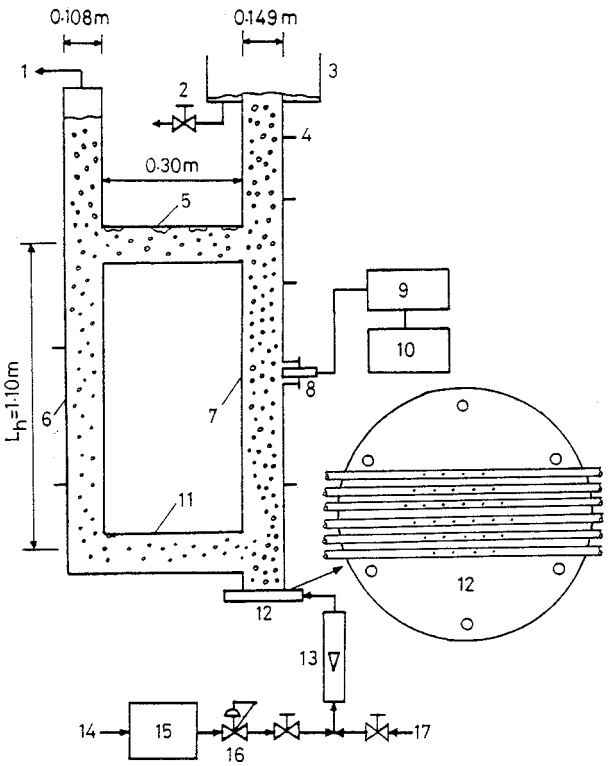

Fig. 1. Schematic diagram of the external-loop airlift reactor.

(1) Vent line
(2) Valve
(3) Wear box
(4) Pressure tap
(5) Top connection
(6) Downcomer
(7) Riser
(8) Dissolved oxygen probe
(9) Dissolved oxygen meter
(10) Wave form analyzer
(11) Bottom connection
(12) Air distributor
(13) Rotameter
(14) Air line
(15) Air filter
(16) Pressure regulator
(17) Nitrogen line

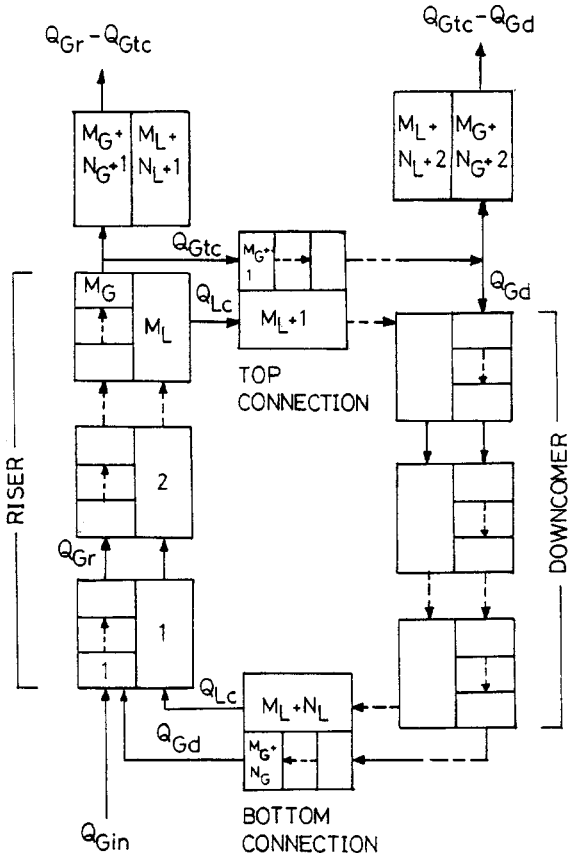

Fig. 2. Block diagram of the unsteady-state model for the airlift reactor.

For simplicity, in this study, it is assumed that the effect of hydrostatic head on the solubility of oxygen is negligible because the airlift reactor is not too tall. The overall volumetric mass transfer coefficient is also assumed to be uniform. In addition, the gas holdup is assumed to be uniform within individual regions. It is very difficult to measure the gas holdups in the top section above the downcomer, the top connection, and the bottom connection. The gas holdup in the top section above the downcomer is assumed to be equal to that in the top connection. The gas holdup in the bottom connection is assumed to be equal to that in the downcomer.

Under unsteady-state conditions, the oxygen balance on the 1st stage of the gas phase in the riser leads to

$$\frac{dC_{G,1}}{dt}=\frac{\gamma_r(Q_{Gin}C_{Gin}+Q_{Gd}C_{G,M_G+N_G}-Q_{Gr}C_{G,1})}{\varepsilon_r V_{ri}} -K_L a_L\frac{(1-\varepsilon_r)}{\varepsilon_r}(C^*_{L,1}-C_{L,1}) \quad (2)$$

where

$$C_G=\frac{P\cdot Y_{O_2}}{RT} \quad (3)$$

$$\gamma_r = \frac{M_L}{M_G} \tag{4}$$

$$V_{ri} = \frac{V_r}{M_L} \tag{5}$$

$$Q_{Gr} = Q_{Gin} + Q_{Gd} \tag{6}$$

According to Henry's law, the partial pressure of oxygen in the gas phase at equilibrium is proportional to the concentration of oxygen in the liquid film:

$$C_L^* = \frac{P_{O_2}}{H} = \frac{C_G RT}{H} \tag{7}$$

In addition, $\overline{C}_{L,i}^*$ represents the average concentration that would be in equilibrium with those stages in the gas phase directly in contact with the ith liquid stage:

$$\overline{C}_{L,i}^* = \frac{\gamma RT}{H} \sum_{j=(i-1)\gamma+1}^{i\gamma} C_{G,j} \tag{8}$$

For the 1st stage of the liquid phase in the riser,

$$\frac{dC_{L,1}}{dt} = \frac{Q_L(C_{L,M_L+M_L} - C_{L,1})}{V_{ri}(1-\varepsilon_r)} + K_L a_L(\overline{C}_{L,1}^* - C_{L,1}) \tag{9}$$

The balance on the ith gas stage in contact with the jth liquid stage in the riser gives the following differential equation :

$$\frac{dC_{G,i}}{dt} = \frac{\gamma_r Q_{Gr}(C_{G,i-1} - C_{G,i})}{\varepsilon_r V_{ri}} - K_L a_L \frac{(1-\varepsilon_r)}{\varepsilon_r}(C_{L,i}^* - C_{L,j}) \tag{10}$$

For the ith stage of the liquid phase in the riser,

$$\frac{dC_{L,i}}{dt} = \frac{Q_L(C_{L,i-1} - C_{L,i})}{V_{ri}(1-\varepsilon_r)} + K_L a_L(\overline{C}_{L,i}^* - C_{L,i}) \tag{11}$$

The top section above the riser is modeled by a well-mixed tank. For the gas phase in the section,

$$\frac{dC_{G,M_G+N_G+1}}{dt} = \frac{(Q_{Gr} - Q_{Gtc})(C_{G,M_G} - C_{G,M_G+N_G+1})}{\varepsilon_{tr} V_{tr}} - K_L a_L \frac{(1-\varepsilon_{tr})}{\varepsilon_{tr}}(C_{G,M_G+N_G+1}^* - C_{L,M_L+N_L+1}) \tag{12}$$

For the liquid phase,

$$\frac{dC_{L,M_L+N_L+1}}{dt} = K_L a_L(C_{L,M_G+N_G+1}^* - C_{L,M_L+N_L+1}) \tag{13}$$

The mass balance on the ith gas stage in contact with the jth liquid stage in the top connection gives:

$$\frac{dC_{G,i}}{dt} = \frac{\gamma_c Q_{Gtc}(C_{G,i-1} - G_{G,i})}{\varepsilon_{tc} V_{ci}} - K_L a_L \frac{(1-\varepsilon_{tc})}{\varepsilon_{tc}}(\overline{C}_{L,i}^* - C_{L,j}) \tag{14}$$

For the ith stage of the liquid phase in the top connection,

$$\frac{dC_{L,i}}{dt} = \frac{Q_L(C_{L,i-1} - C_{L,i})}{V_{ci}(1-\varepsilon_{tc})} + K_L a_L(\overline{C}_{L,i}^* - C_{L,i}) \tag{15}$$

where

$$\gamma_c = \frac{N_L}{N_G} \tag{16}$$

$$V_{ci} = \frac{V_c}{N_L} \tag{17}$$

The material balances on the ith stages in the downcomer and the bottom connection,

$$\frac{dC_{G,i}}{dt} = \frac{\gamma_c Q_{Gd}(C_{G,i-1} - C_{G,i})}{\varepsilon_d V_{ci}} - K_L a_L \frac{(1-\varepsilon_d)}{\varepsilon_d}(C_{L,i}^* - C_{L,j}) \tag{18}$$

for the gas phase, and

$$\frac{dC_{L,i}}{dt} = \frac{Q_L(C_{L,i-1} - C_{L,i})}{V_{ci}(1-\varepsilon_d)} + K_L a_L(\overline{C}_{L,i}^* - C_{L,i}) \tag{19}$$

for the liquid phase.

The gas-liquid mixture in the top section above the downcomer is modeled by a well-mixed tank. Therefore, two mass transfer balances are written for the top region. They are

$$\frac{dC_{G,M_G+N_G+1}}{dt} = \frac{(Q_{Gtc} - Q_{Gd})(C_{G,N_{Gtu}} - C_{G,M_G+N_G+2})}{\varepsilon_{tc} V_t} - K_L a_L \frac{(1-\varepsilon_{tc})}{\varepsilon_{tc}}(C_{L,M_G+N_G+2}^* - C_{L,M_L+N_L+2}) \tag{20}$$

for the gas phase, and

$$\frac{dC_{L,M_L+N_L+1}}{dt} = K_L a_L(C_{L,M_G+N_G+2}^* - C_{L,M_L+N_L+2}) \tag{21}$$

for the liquid phase.

In order to take account of the time delay of oxygen probe, it is assumed that the oxygen probe system is a first order lag system [Muroyama et al., 1985; Chisti and Moo-Young, 1988; Siegel and Merchuk, 1988; Choi, 1993] :

$$\frac{dC_{Lp,i}}{dt} = \frac{(C_{L,i} - C_{Lp,i})}{t_e} \qquad \text{for } i=1,...,M_L+N_L+2; \tag{22}$$

The initial conditions are :

$$C_{L,i} = C_{Lo} \qquad \text{for } i=1,...,M_L+N_L+2;$$

$$C_{G,j} = \frac{C_{Lo} RT}{H} \qquad \text{for } j=1,...,M_G+N_G+2;$$

$$C_{Lp,i} = C_{Lo} \qquad \text{for } i=1,...,M_L+N_L+2.$$

Eqs. (2)-(22) form a system of $2M_L+2N_L+M_G+N_G+6$ linear first order differential equations with constant coefficients. In order to properly solve the system of differential equations, all other parameters found in this model must be known except $2M_L+2N_L+M_G+N_G+6$ concentration terms. The model equations can be solved by a second order Runge-Kutta method [Andre et al., 1983]. The overall volumetric mass transfer coefficient can be determined by fitting the calculated C_{Lp} to the experimentally determined transition curve.

EXPERIMENTAL

Fig. 1 shows a schematic diagram of the external-loop airlift reactor used in this study. The airlift vessel was made of acrylic transparent pipe with 6 mm thickness and aerated liquid heights were kept at 1.77 m. Tap water and air were used as the liquid and gas phases in the experiments. All experiments were carried out at ambient temperature and atmospheric pressure. Filtered air was fed into the riser section through a gas distributor. The air distributor consisted of six tube spargers which were attached on the base plate. Each tube has several 1 mm diameter holes and the

Table 1. Experimental conditions and the dimensions of the experimental apparatus

Riser i.d.	0.149 m
Downcomer i.d.	0.108 m
Connection i.d.	0.108 m
Connection length	0.30 m
Wear box	0.108×0.200×0.300 m
Height between top and bottom connections	1.10 m
Gas phase and liquid phase	air and tap water
Aerated liquid height	1.77 m
Inlet superficial gas velocity	0.02-0.18 m s^{-1}

whole 30 holes of the spargers were arranged in a triangular pitch of 21 mm. Air flow rates were controlled by a precalibrated rotameter. Experimental conditions and the dimensions of the experimental equipment are listed in Table 1.

To determine the overall volumetric oxygen transfer coefficient, K_La_L, a transient dissolved oxygen concentration curve is necessary. First, oxygen in the liquid was purged by dispersing nitrogen gas into the liquid for a certain period of time until the oxygen concentration of the liquid became about 0.3 ppm. After the nitrogen feed was stopped, there was a wait to obtain perfect elimination of nitrogen bubbles from the reactor. Then air was introduced at a constant velocity and the transient dissolved oxygen concentration in the liquid phase was measured with a polarographic probe (Yellow Springs Instruments, YSI 5739 with standard membrane). The signal from the oxygen probe was connected to a YSI model 58 dissolved oxygen meter and simultaneously recorded on a waveform analyzer (Division of Analogic Co., Data 6000 model 611) every 1 s [Choi, 1993]. The oxygen probe was installed at 0.81 m height from the air distributor.

Overall gas holdup was measured by comparison of aerated and unaerated liquid heights. Water manometers were used to obtain gas holdup data in the riser, the downcomer and the top section above the riser. The gas holdup in each section was calculated from the variation of static pressure with height as follows [Hills, 1973].

$$\varepsilon = \frac{\Delta z}{\Delta h} \tag{23}$$

Based on the assumptions that $\varepsilon_{tc}=\varepsilon_{td}$ and $\varepsilon_{bc}=\varepsilon_d$, the gas holdup in the top connection can be determined from the overall gas holdup and other individual gas holdups using the following equation:

$$V_{ov}\varepsilon_{ov} = V_r\varepsilon_r + V_d\varepsilon_d + V_{tr}\varepsilon_{tr} + V_{td}\varepsilon_{td} + V_{tc}\varepsilon_{tc} + V_{bc}\varepsilon_{bc} \tag{24}$$

For the measurement of circulation liquid velocities, 10 mL of 4 M potassium chloride solution was used as a tracer. The response of a pulse input of the tracer was measured by a conductance probe and a conductance meter (YSI model 32) and was simultaneously stored on a wave form analyzer (Division of An-alogic Co., Data 6000 model 611). The circulation liquid velocity was determined from the circulation time, the individual gas holdups, and the reactor's dimensions [Choi, 1996]. The exiting gas rate from the top section above the downcomer, Q_{Gd}, was measured by a bubble flow mater connected to the vent line.

The electrode response time of the dissolved oxygen probe was measured. The electrode response time was determined by the amount of time required to record 63.2 % of the step input value as an electrode reading [Siegel and Merchuk, 1988]. A step change could be made by moving the probe from a reservoir containing oxygen-free water to a reservoir containing water saturated with air at the same temperature. The two reservoirs were well stirred. The average electrode response time was found to be 12.3 s.

RESULTS AND DISCUSSION

In Fig. 3, the transient dissolved oxygen concentration measured by a polarographic probe is represented as a function of the inlet superficial gas velocity. The higher the gas velocity was, the faster the concentration reached to the equilibrium concentration. The rate of approach to new equilibrium depends on the average value of K_La_L in the system. Therefore, the results can be explained by the fact that the larger oxygen transfer coefficients were obtained at the higher gas velocities.

Numerical values of several constants had to be adopted in order to perform the computer simulation. From the data reported by Perry [1984], the following relation may be obtained, which links H with T :

$$H = 4.163\times10^{-4}T - 0.0997 \tag{25}$$

The gas circulation rate in the downcomer was taken from data obtained in an external-loop airlift reactor with an additional gas-liquid separator by Choi [1997], and can be expressed as a function of the downcomer gas holdup as follows:

$$U_{Gd} = 0.3231\varepsilon_d - 0.00007 \tag{26}$$

$$Q_{Gd} = U_{Gd}A_d \tag{27}$$

Parameter values used for computer simulation and the values of K_La_L calculated by using the present model are shown in Table 2. The overall volumetric mass transfer coefficients obtained by the well-mixed model (Eq. (1)), i.e., $(K_La_L)_{wm}$, are also shown in Table 2.

Fig. 4 and Fig. 5 show the comparison of the calculated C_{Lp} and

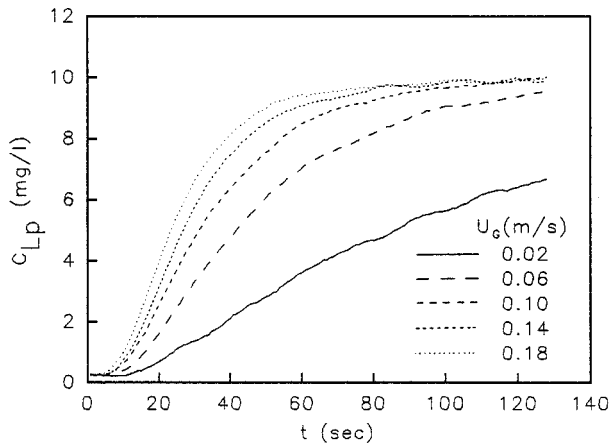

Fig. 3. Effect of U_G on transient dissolved oxygen concentration measured by a polarographic probe.

Table 2. Parameter values used for computer simulation and the calculated values of K_La_L

U_G	ε_{tr}	ε_r	ε_d	ε_{tc}	U_{Lr}	t_c	T	$Q_{Gd}\times10^6$	$K_La_L^*$	$(K_La_L)_{wm}$
0.02	0.0584	0.0427	0.0005	0.0399	0.212	9.27	290.2	78.94	0.0146	0.0097
0.06	0.0985	0.0839	0.0090	0.0866	0.269	7.07	290.3	433.51	0.0319	0.0269
0.10	0.1325	0.1114	0.0250	0.1314	0.282	6.58	290.4	720.53	0.0504	0.0404
0.14	0.1535	0.1330	0.0390	0.1626	0.290	6.27	290.9	927.61	0.0709	0.0517
0.18	0.1650	0.1459	0.0565	0.1885	0.293	6.09	291.0	1055.04	0.0939	0.0634

*Obtained by the present model (M_L=1, M_G=1, N_L=20, N_G=20, ΔT=0.04 s).

the measured C_{Lp} for U_G=0.10 m s^{-1} and U_G=0.14 m s^{-1}, respectively. In Fig. 4 and Fig. 5, we also represented the transition curve of the probe response calculated by the well-mixed model. Fig. 4 and Fig. 5 indicate that the present model shows a better agreement with experimental results than the well-mixed model. The model developed here has much more adjustable parameters, such as M_L, N_L, M_G and N_G, which enables the model to fit available experimental data than the well-mixed model. It means that the present model can be used for the determination of mass transfer performance of the airlift reactor in which the assumption of well-mixed liquid phase is not valid.

The number of mixing stages can be adjusted based on the extent of axial dispersion. The axial dispersion in the gas phase can be different from the axial dispersion in the liquid phase. In this study, the selected values of the parameters were 1, 5, 10 and 20. $N_L \geq M_L$, $N_G \geq M_G$, $M_G \geq M_L$, and $N_G \geq N_L$ were assumed. Warneck et al. [1985] reported that the axial liquid dispersion coefficient of the riser was larger than that of the downcomer in a liquid jet loop reactor. Table 3 shows the effects of those parameters on the standard deviation for U_G=0.10 m s^{-1}. As shown in Table 3, the smallest value of the standard deviation was obtained when M_L=1, M_G=1, N_L=20, and N_G=20. The smallest value of the standard deviation means that those parameters gave the best fitting of the C_{Lp} calculated by the model to the experimentally determined transition curve. At the other values of U_G, the smallest value of the standard deviation was also obtained when M_L=1, M_G=1, N_L=20, and N_G=20.

On the other hand, Andre et al. [1983] reported that a safe criterion for assuming a well-mixed liquid phase in semi-batch liquid contactors would be :

$$(K_La_L)_{wm}\cdot t_c \leq 2 \quad (28)$$

In this work, $(K_La_L)_{wm}\cdot t_c$ was varied in the range of 0.0899-0.386 (Table 2). However, there was a large difference between K_La_L values used in the two models for best fitting. It means that Eq. (28) should be used with caution when the role of the other sections except the riser in the mass transfer is not negligible. At a certain gas velocity, the K_La_L value obtained by the present model was 16-34 % higher than that obtained by the well-mixed model (Table 2). It is evident that the calculated value of the mass transfer coefficient depends on the choice of model. The choice of model is very important because poor assumptions of hydrodynamic characteristics of the equipment may lead to erroneous results.

Fig. 6 shows the effect of the stage number on the actual dissolved oxygen concentration calculated by the present model.

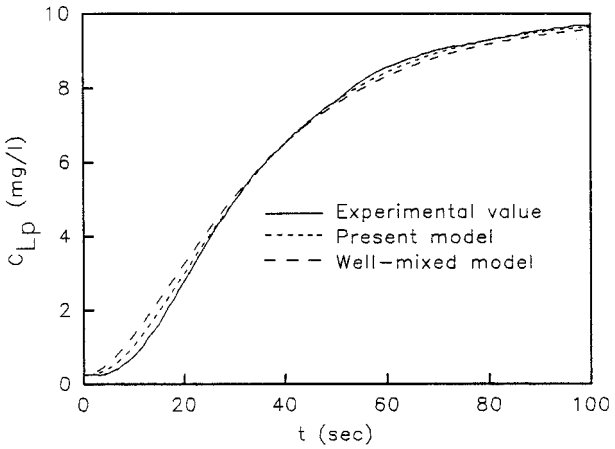

Fig. 4. Comparison of the calculated C_{Lp} and the experimental value.
U_G=0.10 m s^{-1}, M_L=1, M_G=1, N_L=20, N_G=20, ΔT=0.04 s.

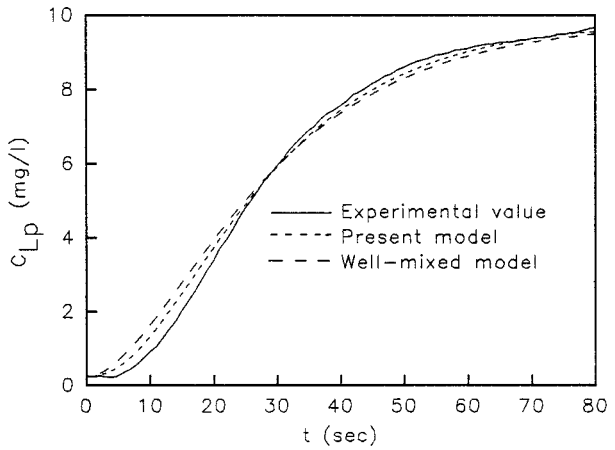

Fig. 5. Comparison of the calculated C_{Lp} and the experimental value.
U_G=0.14 m s^{-1}, M_L=1, M_G=1, N_L=20, N_G=20, ΔT=0.04 s.

Until it became 7 s, which was about the circulation time, there was a variation in the actual dissolved oxygen concentration with the stage number because of both the difference in the extent of oxygen absorption and the effect of the back-mixing of the liquid phase. After 7 s the actual dissolved oxygen concentration was fairly uniform through the reactor.

Probe response dynamics has an influence on the measured values of the dissolved oxygen concentration. Especially, probe response dynamics will become a strong factor when the value

Table 3. Effects of M_L, M_G, N_L and N_G on K_La_L. UG=0.10 m s–1, ΔT =0.04 s

M_L	M_G	N_L	N_G	S.D.	K_La_L	M_L	M_G	N_L	N_G	S.D.	K_La_L
1	1	1	1	0.1565	0.0455	1	10	20	20	0.1363	0.0491
1	1	1	5	0.1298	0.0503	1	20	1	20	0.1521	0.0483
1	1	1	10	0.1299	0.0499	1	20	5	20	0.1390	0.0490
1	1	1	20	0.1301	0.0497	1	20	10	20	0.1379	0.0490
1	1	5	5	0.1179	0.0511	1	20	20	20	0.1374	0.0490
1	1	5	10	0.1184	0.0506	5	5	5	5	0.1303	0.0500
1	1	5	20	0.1187	0.0503	5	5	5	10	0.1311	0.0496
1	1	10	10	0.1174	0.0506	5	5	5	20	0.1316	0.0493
1	1	10	20	0.1178	0.0503	5	5	10	10	0.1299	0.0496
1	1	20	20	0.1173	0.0504	5	5	10	20	0.1305	0.0493
1	5	1	5	0.1482	0.0492	5	10	5	10	0.1332	0.0494
1	5	1	10	0.1482	0.0487	5	10	5	20	0.1338	0.0492
1	5	1	20	0.1484	0.0485	5	10	10	10	0.1320	0.0495
1	5	5	5	0.1349	0.0499	5	10	10	20	0.1326	0.0492
1	5	5	10	0.1353	0.0494	5	10	20	20	0.1321	0.0492
1	5	5	20	0.1356	0.0492	5	20	5	20	0.1348	0.0491
1	5	10	10	0.1342	0.0495	5	20	10	20	0.1337	0.0491
1	5	10	20	0.1345	0.0492	5	20	20	20	0.1332	0.0492
1	5	20	20	0.1340	0.0492	10	10	10	10	0.1289	0.0495
1	10	1	10	0.1507	0.0486	10	10	10	20	0.1296	0.0493
1	10	1	20	0.1508	0.0484	10	10	20	20	0.1291	0.0493
1	10	5	10	0.1375	0.0493	10	20	10	20	0.1307	0.0492
1	10	5	20	0.1379	0.0491	10	20	20	20	0.1302	0.0492
1	10	10	10	0.1364	0.0493	20	20	20	20	0.1286	0.0493
1	10	10	20	0.1368	0.0491						

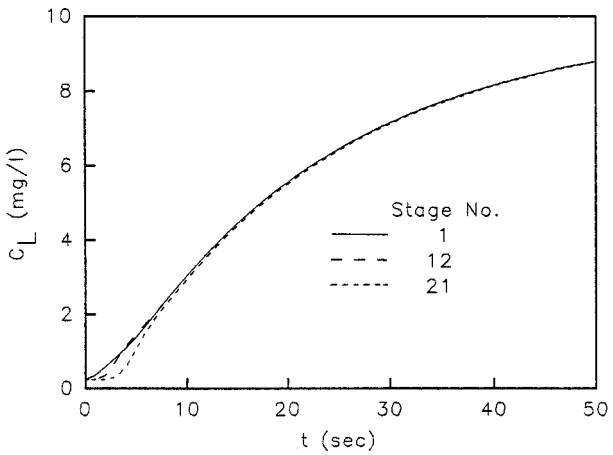

Fig. 6. Effect of stage number on the actual dissolved oxygen concentration in the liquid phase.
U_G=0.10 m s^{-1}, M_L=1, M_G=1, N_L=20, N_G=20, ΔT=0.04 s.

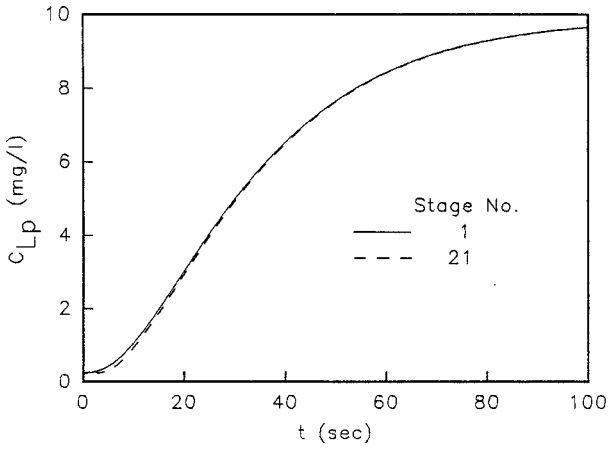

Fig. 7. Simulation results for the variation of the dissolved oxygen concentration measured by oxygen probe with time as a function of the stage number.
U_G=0.10 m s^{-1}, M_L=1, M_G=1, N_L=20, N_G=20, ΔT=0.04 s.

for K_La_L is equal to or greater than the inverse of the probe response time. Fig. 7 shows the simulation results for the variation of the dissolved oxygen concentration measured by oxygen probe with time as a function of the stage number. Comparison of these results with those in Fig. 6 shows that the C_{Lp} calculated by the model had a small variation with the stage number for the initial time (t≅0-7 s) because of the probe response dynamics. These results indicate that the dissolved oxygen concentration measured by the probe was fairly uniform throughout the reactor. Similar results were previously observed by Choi [1989] in the same airlift reactor and by Chisti and Moo-Young [1988] in a rectangular airlift reactor with about 100 L working volumes. So they used the well-mixed model for the determination of oxygen mass transfer coefficients in their reactors. Comparing Fig. 7 with Fig. 6 indi-

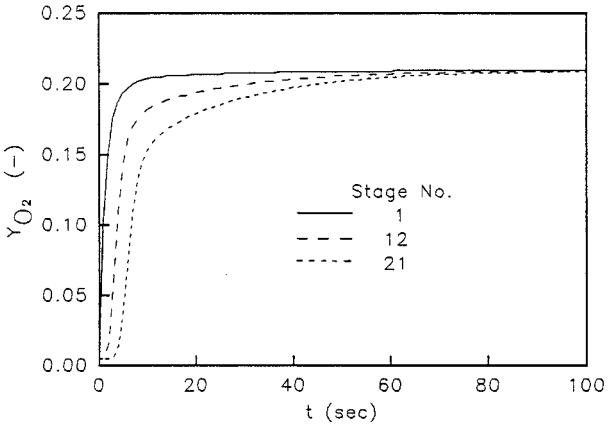

Fig. 8. Simulation results for the variation of oxygen mole fraction in the gas phase with time as a function of stage number.
U_G=0.10 m s^{-1}, M_L=1, M_G=1, N_L=20, N_G=20, ΔT=0.04 s.

cates that the probe response time must be considered for the determination of oxygen mass transfer coefficients under unsteady-state operation.

Fig. 8 shows the simulation results for the variation of oxygen mole fraction in the gas phase with time as a function of the stage number. The results show that there was a large deviation between the oxygen mole fractions in the gas stages. The smaller the stage number was, the faster the oxygen mole fraction in the gas phase increased with time. As compared with the dissolved oxygen concentration in the liquid phase (Fig. 6), the oxygen mole fraction in the gas phase was not uniform through-out the reactor for a longer time because the gas circulation rate was very smaller than the liquid circulation rate for the experiment.

The present model has the following advantages. Since the well-mixed tanks for the downcomer, the connections, and the top section above the downcomer were omitted in the model developed by Andre et al. [1983], the model could not effectively describe the role of those sections in the mass transfer and the mixing. However, the present model considers the role of those sections in the mass transfer and the mixing. Therefore, the present model can be safely applied to the airlift reactor in which both the circulation of the gas phase and the role of the other sections except the riser are important. In comparison with the well-mixed model, the present model allows one to calculate the variation of the oxygen concentrations in the gas and liquid phases with position.

CONCLUSIONS

The model presented could predict oxygen concentration profiles in both liquid and gas phases. The simulation results based on the present mathematical model were in a better qualitative agreement with experimental results than those obtained from the well-mixed model. The present model can be used for the determination of mass transfer coefficient in the airlift reactor in which the assumption of well-mixed liquid phase is not valid.

ACKNOWLEDGEMENTS

The present research has been conducted by the Research Grant of Taejon National University of Technology.

NOMENCLATURE

C : concentration of oxygen [mg O_2/L]
H : Henry's law constant [L·atm/mg O_2]
h : height above gas sparger [m]
K_La_L : overall volumetric mass transfer coefficient [s^{-1}]
L_h : height between top and bottom connections [m]
M : number of mixing stages in riser
N : number of mixing stages in circulation loop
P : total pressure [atm]
P_{O_2} : oxygen partial pressure [atm]
Q : flow rate [m^3 s^{-1}]
R : gas constant [L·atm/mg O_2·°K]
S.D. : standard deviation [mg O_2/L]
T : temperature [°K]
t : time [s]
ΔT : step size for 2nd order Runge-Kutta method [s]
t_c : circulation time [s]
t_e : response time of oxygen probe [s]
V : volume [m^3]
U : superficial velocity [m s^{-1}]
Y_{O_2} : mole fraction of oxygen in gas phase
z : height of manometers [m]

Greek Letters

ε : gas holdup
γ : ratio of the number of liquid stages to the number of gas stages

Superscripts

* : at equilibrium
– : average

Subscripts

bc : bottom connection
c : circulation loop
d : downcomer
G : gas
i : ith stage
in : inlet condition
j : jth stage
L : liquid
o : initial condition
ov : overall
p : measured by oxygen probe
r : riser
tc : top connection
td : top section above downcomer
tr : top section above riser
wm : well-mixed liquid phase

REFERENCES

Andre, G., Robinson, C. W. and Moo-Young, M., "New Criteria for Application of the Well-Mixed Model to Gas-Liquid Mass Transfer Studies," *Chem. Engng. Sci*., **38**, 1845 (1983).

Chisti, M. Y. and Moo-Young, M., "Hydrodynamics and Oxygen Transfer in Pneumatic Bioreactor Devices," *Biotechnol. Bioeng*., **31**, 487 (1988).

Choi, K. H., "Circulation Liquid Velocity, Gas Holdup and Volumetric Oxygen Transfer Coefficient in External-Loop Airlift Reactors," *J. Chem. Tech. Biotechnol*., **56**, 51 (1993).

Choi, K. H., "Circulation Liquid Velocity in External-Loop Airlift Reactors," *Korean J. Chem. Eng*., **13**, 379 (1996).

Choi, K. H., "Circulation of Gas and Liquid Phases in External-Loop Airlift Reactors," *Chem. Eng. Comm*., **160**, 103 (1997).

Choi, K. H., "Hydrodynamics and Oxygen Transfer Characteristics in Airlift Bioreactor," Ph.D. thesis, KAIST, Taejon, Korea (1989).

Choi, K. H., Han, B. H. and Lee, W. K., "Effect of Horizontal Connection Pipe Length on Gas Holdup and Volumetric Oxygen Transfer Coefficient in External-Loop Airlift Reactor," *HWAHAK KONGHAK*, **28**, 220 (1990).

Hills, J. H., "The Operation of a Bubble Column at High Throughputs I. Gas Holdup Measurement," *Chem. Eng. J*., **12**, 89 (1973).

Ho, C. S., Erickson, L. E. and Fan, L. T., "Modeling and Simulation of Oxygen Transfer in Airlift Fermentors," *Biotechnol. Bioeng*., **19**, 1503 (1977).

Linek, V. and Sinukle, J., "Comprehensive Biotechnology," Pergamon Press, Oxford, **4**, 363 (1985).

Luttmann, R., Buchholz, H., Zakrzewski, W. and Schügerl, K., "Identification of Mass-Transfer Parameters and Process Simulation of SCP Production Processes in Airlift Tower Reactors with an External Loop," *Biotechnol. Bioeng*., **24**, 817 (1982).

Merchuk, J. C. and Siegel, M. H., "Air-Lift Reactors in Chemical and Biological Technology," *J. Chem. Tech. Biotechnol*., **41**, 105 (1988).

Merchuk, J. C. and Stein, Y., "Distributed Parameter Model of an Airlift Fermenter," *Biotechnol. Bioeng*., **22**, 1189 (1980).

Muroyama, K., Mitani, Y. and Yasunishi, A., "Hydrodynamic Characteristics and Gas-Liquid Mass Transfer in a Draft Tube Slurry Reactor," *Chem. Eng. Commun*., **34**, 87 (1985).

Perry, R. H. and Green, D. W., "Perry's Chemical Engineers Handbook," 6th ed., McGraw-Hill, New York (1984).

Siegel, M. H. and Merchuk, J. C., "Mass Transfer in a Rectangular Air-Lift Reactor: Effects of Geometry and Gas Recirculation," *Biotechnol. Bioeng*., **32**, 1128 (1988).

Weiland, P. and Onken, U., *Ger. Chem. Eng.*, **4**, 42 (1981).

Werneke, H.-J., Prüss, J., Leber, L. and Langemann, H., "On a Mathematical Model for Loop Reactors-II. Estimation of Parameters," *Chem. Eng. Sci*., **40**, 2327 (1985).